

# Coexistence curve of perfluoromethylcyclohexane-isopropyl alcohol

D. T. Jacobs,<sup>a)</sup> D. E. Kuhl,<sup>b)</sup> and C. E. Selby<sup>c)</sup>

*Department of Physics, The College of Wooster, Wooster, Ohio 44691*

(Received 26 February 1996; accepted 3 April 1996)

The coexistence curve of the binary fluid mixture perfluoromethylcyclohexane-isopropyl alcohol was determined by precisely measuring the refractive index both above and below its upper critical consolute point. Sixty-seven two-phase data points were obtained over a wide range of reduced temperatures,  $10^{-5} < t < 2.5 \times 10^{-1}$ , to determine the location of the critical point: critical temperature = 89.901 °C, and critical composition = 62.2% by volume perfluoromethylcyclohexane. These data were analyzed to determine the critical exponent  $\beta$  close to the critical point, the amplitude  $B$ , and the anomaly in the diameter. The volume-fraction coexistence curve is found to be as symmetric as any compositionlike variable. Correction to scaling is investigated as well as the need for a crossover theory. A model is proposed that describes the asymptotic approach to zero of the effective exponent  $\beta$ , which allows an estimation of the temperature regime free of crossover effects. © 1996 American Institute of Physics. [S0021-9606(96)51626-0]

## I. INTRODUCTION

The substantial recent interest in critical phenomena in a multitude of physical systems has been built upon concepts of scaling and universality which developed from studying second-order phase transitions in fluid systems. A framework in renormalization group theory has been used by many others to predict relationships among exponents, the values exponents should have when they belong to different universality classes, and relationships among the amplitudes of thermodynamic quantities. Although renormalization group theory does not predict the location of the critical point, all systems in a given universality class behave similarly once they are close to their own critical points.

The predictions for the exponents have been well verified<sup>1</sup> close to the critical point in liquid-gas systems and close to the critical consolute points in binary fluid mixtures, both of which belong to the same universality class (three-dimensional Ising model). Two-scale-factor universality predicts that two independent amplitudes of leading anomalies (e.g., correlation length and compressibility) can be used to determine amplitudes for other quantities near the critical point. Thus, it is possible to measure thermodynamic quantities in a system to obtain independent amplitudes, and then accurately predict most of the thermodynamic behavior near the critical point for that system. Several reviews discuss<sup>1,2</sup> the present status of experiments and theory in these simple systems. Such systems provide essential models for understanding the behavior near critical points of much more complicated systems, such as polymer-solvent phase separation,<sup>3</sup> polymer-polymer blends,<sup>4</sup> ionic systems,<sup>5</sup> micelles,<sup>6</sup> etc.

In order to determine critical amplitudes and exponents, it is essential to be near the critical point. The coexistence curve provides the location of the critical point and is the

first experiment that must be conducted on a system. The shape of the coexistence curve has traditionally provided information on the critical exponent  $\beta$  and amplitude  $B$ . This arises from simple scaling, where the difference in order parameter  $x$  between the upper ( $u$ ) and lower ( $l$ ) phases goes as a simple power law in reduced temperature  $t \equiv (T_c - T)/T_c$  when very close to the critical temperature  $T_c$ :

$$\Delta x \equiv x_u - x_l = B t^\beta \quad (\text{simple scaling}). \quad (1)$$

Further from the critical point, additional, “correction-to-scaling” or Wegner,<sup>1,2</sup> terms are needed:

$$\Delta x = B t^\beta [1 + B_1 t^{\Delta_1} + B_2 t^{2\Delta_1} + \dots], \quad (2)$$

where the amplitudes  $B$ ,  $B_1$ , etc., are system dependent, but the exponent  $\Delta_1$  is predicted<sup>1,2</sup> to be a universal 0.51. The critical exponent,  $\beta$ , is predicted<sup>1,2</sup> to be  $0.327 \pm 0.002$ . Singh and Pitzer<sup>7</sup> have looked at a number of binary fluid mixtures and concluded that, experimentally, upper consolute points have correction-to-scaling amplitudes  $B_1 = 0$ , while  $B_2$  is negative and system dependent.

The theory describing a system very far from the critical point is less certain. Recent work<sup>8</sup> has focused on the global region containing a critical point and the substantial influence of the critical point on the observed behavior. Crossover theories have been developed<sup>8</sup> for liquid-gas critical points that allow two distinct critical points: one describes the near-critical, Ising-like behavior, which crosses over to the mean-field critical point when the system is far from the Ising critical point. Corresponding theories for binary fluid mixtures near their critical consolute point are under development.<sup>9</sup> Testing these theories requires precise data over a broad range of temperatures in a variety of systems, which we have continued to acquire with the system reported here.

In liquid-gas systems, the order parameter is the density,<sup>1,2</sup> for binary fluid mixtures the proper order parameter is still uncertain, although many favor volume fraction since this gives<sup>1,2,5</sup> a more symmetric Ising-like coexistence

<sup>a)</sup> Author to whom all correspondence should be addressed.

<sup>b)</sup> Present address: Physics and Astronomy Dept., Michigan State Univ., East Lansing, MI 48824-1116.

<sup>c)</sup> Present address: OSU College of Veterinary Medicine, 0004 Veterinary Hospital, Columbus, OH 43210-1089.

curve. The symmetry of the coexistence curve in a given composition variable depends on the properties of the pure components. It has been observed<sup>5</sup> that dissimilar components tend to have skewed coexistence curves in any of the traditional composition variables of volume fraction, mass fraction, or mole fraction. While various schemes<sup>3,5,10,11</sup> have been developed to find a composition variable that symmetrizes the coexistence curve, none have been wholly successful.

The experimental study of binary liquid mixtures near their critical consolute point has several advantages over liquid-gas systems. A binary liquid mixture has a critical point at atmospheric pressure, can have a critical temperature close to room temperature, has minimal gravity effects, and typically obeys simple scaling for relatively large reduced temperatures.<sup>1,2</sup> Moreover, more complex systems that involve mixtures can be modeled in the simpler binary liquid systems by choosing components appropriately.

While the coexistence curve of a binary liquid mixture can be measured by several techniques,<sup>2</sup> the one utilized in this experiment is to measure the refractive index of a sealed sample at various temperatures,<sup>12,13</sup> which provides a measure of the composition of each phase. The refractive index is a precise, nonintrusive probe which can measure the properties of the coexisting phases for a single sample of fixed composition. Investigating one sample avoids the problem of preparing multiple samples without introducing differing amounts of impurities, which affect the critical temperature and critical composition.<sup>14</sup>

The volume fraction of component 1 in a phase can be calculated from the refractive index of that phase using two assumptions. First, that the refractive index itself does not have a significant anomaly close to a critical point; measurements and predictions<sup>15</sup> show any such anomaly to be smaller than the resolution in this experiment. Second, that the Lorentz-Lorenz relation holds for binary liquid mixtures. Direct experimental tests<sup>13,16,17</sup> of the Lorentz-Lorenz relation in near-critical binary fluid mixtures have verified the Lorentz-Lorenz relation within experimental error (0.5%). Until a proper order parameter is established for binary liquid mixtures, the choice of composition variable is still somewhat arbitrary<sup>1,2</sup> so that other "composition" variables can also be used in analyzing our data.

This experiment uses refractive index techniques to investigate the coexistence curve of the binary fluid mixture perfluoromethylcyclohexane-isopropyl alcohol (PFMC-IPA). This coexistence curve has not been precisely measured<sup>18</sup> over an extended temperature region before, yet provides an intriguing system because of the high critical temperature and of the mismatch of the components (PFMC-IPA) has a density ratio of 2.27 and molecular weight ( $M_w$ ) ratio of 5.82), which results in a skewed coexistence curve over an extended temperature region. Thus, issues of crossover and coexistence curve symmetry can be investigated.

## II. EXPERIMENT

The fluids were spectral grade isopropyl alcohol (Fisher's Spectranalyzed), used without further purification,

and perfluoromethylcyclohexane (PCR, >97% pure), which was distilled in a spinning band still with a reflux ratio of 20:1 to achieve a purity greater than 99.9%, as determined by a gas chromatograph. The fluids were transferred in a dry box under a nitrogen atmosphere to prevent further water contamination. The refractive index and density of the pure components were measured independently. The refractive index was determined using the equipment described below at a wavelength of 632.8 nm with the values for pure PFMC fitted by  $n_1 = 1.2877 - 3.977 \times 10^{-4}T - 6.64 \times 10^{-7}T^2$ , while values for pure IPA were fitted by  $n_2 = 1.3827 - 3.861 \times 10^{-4}T - 8.47 \times 10^{-7}T^2$ , where  $T$  is in °C. These are consistent with the published<sup>18</sup> values at 90 °C. The densities ( $\text{g/cm}^3$ ) were measured in a temperature controlled ( $\pm 1$  mK), vibrating tube densimeter<sup>19</sup> and found to be described by  $\rho_1 = 1.8490 - 2.460 \times 10^{-3}T - 3.79 \times 10^{-6}T^2$  for PFMC and  $\rho_2 = 0.80034 - 7.035 \times 10^{-4}T - 2.55 \times 10^{-6}T^2$  for IPA.

One composition of the fluid mixture was prepared and measured: 53.1% by volume PFMC, which was reported by Schmidt<sup>18</sup> as the critical composition. The mixture was sealed in a stainless steel, prism-shaped cell<sup>12</sup> that has a volume of 7.1 cm<sup>3</sup>, including a 0.6 cm<sup>3</sup> nitrogen bubble to maintain the pressure close to atmospheric. The fluids were sealed with indium wire o-rings for the windows and a Teflon™ plug on the fill-hole, sealing screw. The cell temperature was controlled with an ac Wheatstone bridge using a seven digit ratio transformer (General Radio 1493A) and lock-in amplifier (EG&G 128A). A temperature controlled thermostat surrounded the cell as before,<sup>12</sup> and included an outer stage with attached copper tubing through which a circulating antifreeze-water mixture could flow from a water bath (Lauda RM-6). The cell temperature was sensed by a Thermometrics ultrastable thermistor which was calibrated to 0.01 K. Temperature resolution was  $\pm 0.2$  mK with control of  $\pm 0.5$  mK over 24 h.

The bulk refractive index was determined from measurements of the minimum deviated angle of 632.8 nm He-Ne laser light bending through each phase of the prism-shaped sample of fluid. The undeviated angle and the prism angle were also measured. Angles were read with a Gaertner spectrometer to a precision of 20 arcsec, providing a resolution in refractive index of  $\pm 0.0001_5$ . The procedure for taking a data point and calculating the refractive index is the same as reported previously.<sup>12</sup> After temperature control was achieved for each data point, the thermostat was shaken to mix the fluids across the meniscus and to prevent gravitational stratification<sup>2</sup> from occurring. The fluids showed wetting behavior<sup>20</sup> at temperatures below 50 °C but not at temperatures closer to critical. The wetting behavior consisted of the lower phase wetting the inside of the container and surrounding the upper phase with a thin (and for this experiment, unmeasurable) film that caused a tiny pendent droplet to form at the interface between the upper phase and the nitrogen bubble. Previous publications<sup>20</sup> have measured the wetting phenomena in this system.

A weighted, nonlinear, least-squares routine was used to fit the equations to the data by finding the best set of param-

eters that minimizes<sup>21</sup> the reduced chi-square  $\chi^2/N$ . Using our own functions in the commercial program IGOR PRO,<sup>22</sup> we could allow some parameters to be free and force others to take on certain values as will be described below. This program allows each data point to be weighted according to the error in the dependent variable and determines errors on the parameters that are related to the diagonal elements of the typical error matrix.<sup>21</sup> While this is adequate for equations whose parameters enter linearly, errors of nonlinear parameters should be determined by error ellipses.<sup>23</sup> In tests on a subset of this data against a program<sup>24</sup> that correctly determines the errors, we found that the parameter values were consistent, and that the IGOR errors exceeded the appropriate, one standard deviation ( $1\sigma$ ) errors. In the following, our quoted parameter errors are those given by the program and should be considered the  $1\sigma$  error.

### III. RESULTS

Data were taken in two runs over a several month period, and the data spanned over five decades in reduced temperature  $1 \times 10^{-5} < (T_c - T)/T_c < 2.6 \times 10^{-1}$ . The critical temperature was observed visually for each run to be  $89.901 \pm 0.0005$  °C. The raw refractive index data were reproducible and are listed in Table I and shown in Fig. 1 without distinction. The coexistence curve appears quite skewed in Fig. 1 because the two phases separate into essentially the pure components within the region studied. Thus, the sides of the coexistence curve, as represented by the refractive index, asymptotically approach the pure component refractive index temperature dependence as is shown in Fig. 1. The average of the upper and lower phase refractive indices represents the "diameter" of the coexistence curve. The diameter can be extrapolated to the critical temperature and compared to the one-phase values to give a correction to the critical composition; these data show no measurable difference between the one-phase and diameter refractive index at the critical point. This means that the composition of 53.1% by volume PFMC, which is prepared at room temperature, results in the critical composition when the system is at the critical temperature. Our measured refractive index values are also consistent with Schmidt's measurement of the refractive index, which was reported<sup>18</sup> as an equation and is compared to our data in the inset of Fig. 1.

Using the densities ( $\rho_1$  and  $\rho_2$ ) and the refractive indices reported above for the pure components, the effectively constant polarizabilities  $\alpha_1 = 0.0233$  and  $\alpha_2 = 0.0700$  cm<sup>3</sup>/g can be determined and used to calculate the volume fraction  $\phi_1$  from the Lorentz-Lorenz relation.<sup>16</sup>

$$\begin{aligned} \frac{n^2 - 1}{n^2 + 2} &= \frac{4\pi}{3} (\alpha_1 \rho_1 \phi_1 + \alpha_2 \rho_2 \phi_2) \\ &= \frac{4\pi}{3} (\alpha_2 \rho_2 + (\alpha_1 \rho_1 - \alpha_2 \rho_2) \phi_1), \end{aligned} \quad (3)$$

where 1 and 2 refer to PFMC and IPA, respectively. The resulting values are listed in Table I and shown in Fig. 2. Two trends are immediately apparent: (1) the mixture phase

TABLE I. The coexistence curve data for the critical concentration of perfluoromethylcyclohexane-isopropyl alcohol in both the two- and one-phase regions. The measured data were of the refractive index  $n$ , while the volume fraction  $\phi$  is calculated using the Lorentz-Lorenz relation as described in the text. The critical temperature was observed to be 89.901 °C.

2 phase				
Temperature	$n$		$\phi$	
	lower phase	upper phase	lower phase	upper phase
89.9009	1.2808	1.2823	0.6312	0.6152
89.9004	1.2806	1.2826	0.6334	0.6120
89.9000	1.2797	1.2833	0.6430	0.6046
89.8994	1.2802	1.2829	0.6376	0.6088
89.8984	1.2797	1.2836	0.6430	0.6014
89.8978	1.2797	1.2838	0.6430	0.5993
89.8972	1.2795	1.2840	0.6451	0.5972
89.8966	1.2793	1.2841	0.6472	0.5961
89.8962	1.2796	1.2841	0.6440	0.5961
89.8962	1.2792	1.2844	0.6483	0.5929
89.8939	1.2793	1.2844	0.6473	0.5929
89.8939	1.2789	1.2842	0.6515	0.5950
89.8929	1.2791	1.2847	0.6494	0.5897
89.8919	1.2789	1.2847	0.6515	0.5897
89.8909	1.2785	1.2845	0.6558	0.5919
89.8907	1.2788	1.2851	0.6526	0.5855
89.8896	1.2786	1.2853	0.6548	0.5834
89.8894	1.2783	1.2853	0.6580	0.5834
89.8888	1.2783	1.2849	0.6580	0.5876
89.8876	1.2786	1.2849	0.6548	0.5876
89.8870	1.2787	1.2847	0.6537	0.5898
89.8860	1.2785	1.2849	0.6558	0.5876
89.8850	1.2785	1.2847	0.6558	0.5898
89.8841	1.2781	1.2857	0.6601	0.5791
89.8752	1.2776	1.2862	0.6655	0.5739
89.8640	1.2771	1.2862	0.6709	0.5739
89.8512	1.2762	1.2876	0.6806	0.5591
89.8251	1.2748	1.2893	0.6957	0.5413
89.8172	1.2752	1.2882	0.6915	0.5530
89.8105	1.2737	1.2897	0.7076	0.5371
89.6839	1.2719	1.2910	0.7276	0.5240
89.6735	1.2723	1.2918	0.7234	0.5156
89.4146	1.2703	1.2945	0.7463	0.4885
89.3764	1.2695	1.2942	0.7551	0.4919
88.8643	1.2668	1.2979	0.7869	0.4556
88.8643	1.2679	1.2983	0.7751	0.4514
87.8394	1.2644	1.3025	0.8185	0.4129
85.8030	1.2623	1.3090	0.8525	0.3558
85.8029	1.2616	1.3090	0.8600	0.3558
85.7507	1.2621	1.3090	0.8549	0.3561
83.7434	1.2603	1.3133	0.8855	0.3221
80.6858	1.2598	1.3192	0.9077	0.2771
78.6429	1.2596	1.3219	0.9210	0.2600
75.5850	1.2600	1.3266	0.9333	0.2274
73.5170	1.2601	1.3286	0.9433	0.2176
70.4982	1.2609	1.3327	0.9508	0.1909
68.6047	1.2613	1.3342	0.9565	0.1852
63.4007	1.2629	1.3392	0.9666	0.1602
60.3544	1.2639	1.3420	0.9716	0.1467
58.5837	1.2645	1.3434	0.9742	0.1411
52.7777	1.2666	1.3481	0.9811	0.1214
50.2475	1.2679	1.3504	0.9798	0.1101
47.8211	1.2687	1.3519	0.9833	0.1063
43.1878	1.2703	1.3549	0.9890	0.0975
40.1700	1.2719	1.3573	0.9865	0.0871
38.1572	1.2723	1.3581	0.9920	0.0882
34.1374	1.2742	1.3610	0.9908	0.0769
31.3217	1.2759	1.3632	0.9858	0.0671
31.2997	1.2754	1.3630	0.9913	0.0692

TABLE I. (Continued.)

2 phase				
Temperature	$n$ lower phase	$n$ upper phase	$\phi$ lower phase	$\phi$ upper phase
30.1209	1.2760	1.3636	0.9904	0.0684
25.1050	1.2779	1.3662	0.9935	0.0640
23.0860	1.2786	1.3674	0.9953	0.0605
20.0943	1.2803	1.3694	0.9907	0.0530
15.0876	1.2824	1.3720	0.9908	0.0478
10.0847	1.2842	1.3744	0.9937	0.0441
5.0845	1.2864	1.3771	0.9920	0.0369
0.0863	1.2883	1.3793	0.9931	0.0344
1 phase				
91.9376	1.2804		0.6241	
91.8366	1.2804		0.6246	
91.7337	1.2806		0.6231	
91.6312	1.2807		0.6226	
91.5287	1.2808		0.6221	
91.4262	1.2809		0.6216	
91.3229	1.2809		0.6222	
91.2342	1.2809		0.6227	
91.1181	1.2811		0.6212	
91.0159	1.2811		0.6218	
90.9141	1.2812		0.6213	
90.8120	1.2813		0.6208	
90.7085	1.2814		0.6203	
90.6055	1.2814		0.6209	
90.5035	1.2815		0.6204	
90.4004	1.2816		0.6199	
90.2988	1.2817		0.6194	
90.2471	1.2816		0.6208	
90.1962	1.2815		0.6221	
90.1444	1.2817		0.6203	
90.0938	1.2816		0.6216	
90.0936	1.2818		0.6195	
90.0682	1.2818		0.6196	
90.0429	1.2819		0.6187	
90.0225	1.2817		0.6209	
89.9965	1.2817		0.6211	
89.9659	1.2821		0.6170	
89.9298	1.2820		0.6183	
89.9257	1.2816		0.6225	
89.9145	1.2821		0.6173	
89.9094	1.2817		0.6216	
89.9041	1.2820		0.6184	
89.9041	1.2817		0.6216	
89.9031	1.2815		0.6237	
89.9021	1.2815		0.6237	
89.9011	1.2815		0.6238	

separates and those phases asymptotically approach pure components, and (2) the coexistence curve is still asymmetric, which is common when the two components are very dissimilar.<sup>5</sup> A skewed coexistence curve corresponds to a nonlinear diameter.

#### IV. ANALYSIS AND DISCUSSION

The coexistence curve data presented above will be analyzed in four ways. First, the diameter of the volume fraction coexistence curve will be analyzed to look for any anomaly. Second, the shape of the coexistence curve will be studied over different temperature regions to determine the asymp-

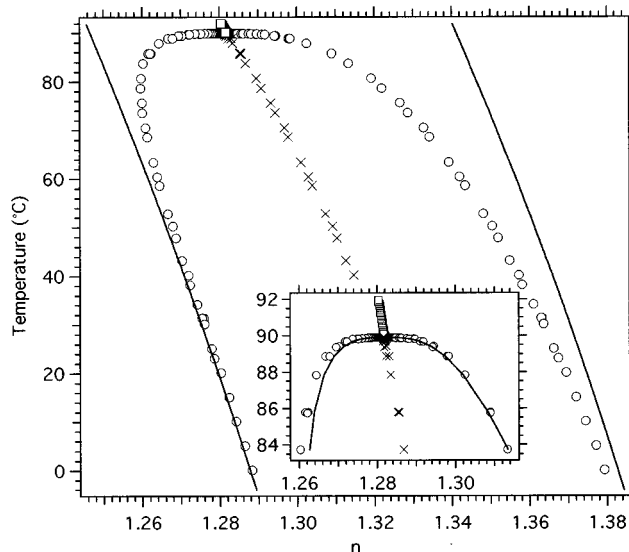


FIG. 1. The refractive index coexistence curve of perfluoromethylcyclohexane-isopropanol. The  $o$ 's are the upper and lower phase refractive index data for the critical composition mixture and the squares are the one-phase data. The average of the upper and lower phase refractive indices are indicated by  $x$ 's and form the diameter of the curve. The long straight lines on either side of the coexistence curve reflect the refractive index behavior for the pure components. In the inset, our coexistence curve data near the critical point are compared to the equation in Ref. 18, which was fitted to their refractive index data for this system.

otic exponent  $\beta$  and the need for correction-to-scaling terms and their amplitude values. Third, the issue of extended scaling versus a crossover expression will be discussed and a simple model will be developed. Fourth, different "composition" variables will be used to determine if the coexistence curve can be symmetrized.

#### A. Diameter

The average of the upper ( $u$ ) and lower ( $l$ ) composition values is referred to as the diameter of the coexistence curve. The diameter  $\bar{x}$  has a power-law dependence with exponent  $\sigma$ ,<sup>1,2</sup>

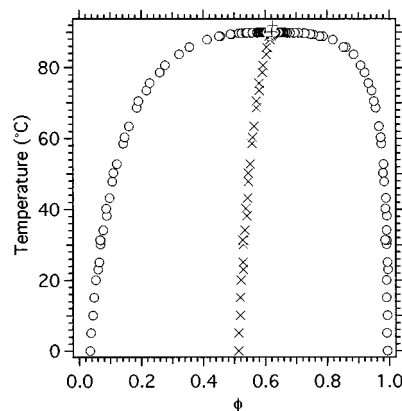


FIG. 2. The coexistence curve plotted with volume fraction as the composition variable. The symbols are the same as in Fig. 1 except the one-phase points, which are indicated by a plus (+) sign. This composition variable provides as symmetric a coexistence curve as any compositionlike variable.

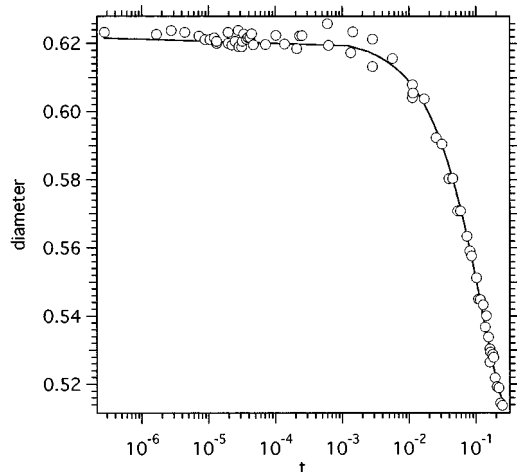


FIG. 3. The diameter of the volume fraction coexistence curve, shown by  $x^*$ 's in Fig. 2, is plotted as a function of reduced temperature  $t = (T_c - T)/T_c$ . The curve is the best fit from Table II.

$$\bar{x} \equiv (x_u + x_l)/2 = x_c + at + At^\sigma(1 + A_1 t^{\Delta_1} + \dots), \quad (4)$$

where  $t$  is the reduced temperature,  $A$  is the amplitude of the leading critical contribution,  $A_1$  is the amplitude of the first correction-to-scaling term, “ $a$ ” is the amplitude of the linear, analytic temperature dependence, and  $\Delta_1$  is the universal exponent ( $\Delta_1 = 0.5$ ). An ideal, symmetric coexistence curve would have  $a = 0$ , and would have an exponent  $\sigma = 1 - \alpha = 0.89$  for the “proper” order parameter, while an “improper” order parameter should have a  $\sigma = 2\beta = 0.65$  instead.<sup>2</sup> We analyzed the diameter of this coexistence curve using volume fraction and found that the data close ( $t < 6 \times 10^{-3}$ ) to the critical point are very symmetric ( $a \approx 0$ ) about the critical composition  $\phi_c = 0.6215 \pm 0.0015$ . A plot of the diameter data and the best fit are shown in Fig. 3. It is possible to fit the diameter over the entire temperature region to an analytic, cubic function (see Table II). However, a  $1 - \alpha$  term, with one correction-to-scaling term, significantly improved the fit using fewer free parameters and without the need of a linear term. A  $2\beta$  term did not fit the data nearly as well. The same result was found over a temperature region closer to critical. The diameter data are consistent with a  $\sigma = 1 - \alpha = 0.89$  dependence, which would indicate that the volume fraction provides a symmetric coexistence curve about the critical composition, and is a proper order parameter in this system.

### B. Exponent $\beta$ from volume fraction coexistence curve

The shape of the coexistence curve is expected to be a simple power law in reduced temperature as given by Eq. (1) when the system is sufficiently close to the critical point, and to include correction-to-scaling terms further from the critical point. We will discuss here our fits of Eqs. (1) and (2) to our volume fraction data as given in Table I. Other composition variables will be discussed in a later section. The question of how close one must be to apply Eqs. (1) and (2) will be addressed in the next section in some detail. For now, we

TABLE II. The diameter  $\bar{\phi}$  of the volume fraction. Coexistence curve was fitted by both an analytic (polynomial) function and by the predicted critical point expressions that involve a noninteger power of  $t$ , the reduced temperature. The error in the diameter was taken to be 0.002. An asterisk marks the best fit overall. Errors are one standard deviation; parameters were fixed if no error is given.

$\bar{\phi} = \phi_c + at + bt^2 + ct^3$ (analytic)					
range	$\phi_c$	$a$	$b$	$c$	$\chi^2/N$
$t \leq 3.1 \times 10^{-2}$	0.6213 $\pm 0.0003$	-1.101 $\pm 0.045$	0	0	1.20
$t < 0.26$	0.6204 $\pm 0.0003$	-0.887 $\pm 0.012$	1.94 $\pm 0.06$	0	2.78
	0.6212 $\pm 0.0003$	-1.127 $\pm 0.027$	5.01 $\pm 0.32$	-9.1 $\pm 0.9$	1.30
$\bar{\phi} = \phi_c + At^\sigma + A_1 t^{\sigma + \Delta_1}$ , $\Delta_1 = 0.5$					
range	$\phi_c$	$A$	$A_1$	$\sigma$	$\chi^2/N$
$t \leq 3.1 \times 10^{-2}$	0.6222 $\pm 0.0003$	-0.293 $\pm 0.012$	0	0.65	1.30
	0.6215 $\pm 0.0003$	-0.731 $\pm 0.030$	0	0.89	1.11
$t \leq 0.26$	0.6228 $\pm 0.0003$	-0.373 $\pm 0.009$	0.189 $\pm 0.020$	0.65	1.63
	0.6215 $\pm 0.0003$	-0.863 $\pm 0.016$	0.994 $\pm 0.036$	0.89	1.15*
	0.6218 $\pm 0.0004$	-0.713 $\pm 0.072$	0.74 $\pm 0.12$	0.83 $\pm 0.03$	1.10

will restrict the range in reduced temperature  $t$  over which we fit. Figure 4 gives a sense of the critical region where a straight line can approximate the data. When we look very close to the critical point ( $|t| < 10^{-4}$ ), Eq. (1) fits the data well with an exponent  $\beta$  that is consistent with theoretical predictions, but with amplitudes that are poorly determined (see fit parameters in Table III). As the range is extended ( $|t| < 6 \times 10^{-3}$ ), the exponent tends to be larger which means that the value of the correction-to-scaling term  $B_1$  will be positive when  $\beta$  is fixed at its theoretical value of 0.327. The best fit gives  $B = 2.16 \pm 0.04$  when  $\beta$  is fixed at 0.327. Fol-

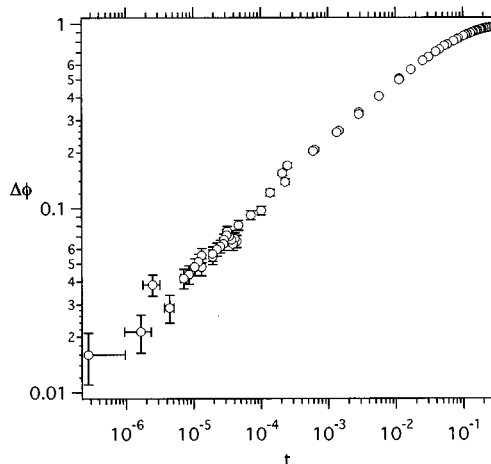


FIG. 4. A log-log plot of the difference in volume fraction between the upper and lower phases as a function of the reduced temperature  $t$ . If simple scaling holds, then the points should fall on a straight line of slope  $\beta$ . The effective slope asymptotically approaches zero at large  $t$ .

TABLE III. Parameter values corresponding to the best fit of  $\phi = \phi_c + at \pm (B/2)t^\beta(1 + B_1t^{\Delta_1})$  to the volume fraction data in Table I.  $N$  is the number of points and  $\chi^2/N$  is the chi square per point. The best fit is marked with an asterisk.

Fit	Region	$N$	$\phi_c$	$a$	$B$	$B_1$	$\beta$	$\chi^2/N$
A	$ t  \leq 10^{-4}$	52	0.6215 $\pm 0.0007$	0	1.88 $\pm 0.58$	0	0.322 $\pm 0.009$	0.28
B	$ t  \leq 6 \times 10^{-3}$	74	0.6210 $\pm 0.0006$	0	2.206 $\pm 0.018$	0	0.327	1.01
C			0.6215 $\pm 0.0006$	-1.11 $\pm 0.52$	2.206 $\pm 0.018$	0	0.327	0.96
D			0.6215 $\pm 0.0006$	-1.11 $\pm 0.52$	3.56 $\pm 0.38$	-2.7 $\pm 0.9$	0.38 $\pm 0.01$	0.67
E*			0.6215 $\pm 0.0006$	-1.11 $\pm 0.52$	2.160 $\pm 0.036$	0.51 $\pm 0.34$	0.327	0.94*

lowing the suggestion of Singh and Pitzer,<sup>7</sup> we also tried a fit over this region when  $B_1=0$  and  $B_2$  was free, but the resulting fit was worse than the ones in Table III.

### C. Crossover vs. correction to scaling

Correction-to-scaling terms allow the Ising critical region to be extended. However, at some point the system will crossover to a mean-field critical point, as has been shown in liquid-vapor systems.<sup>8</sup> This does not mean that the critical exponent  $\beta$  will crossover from Ising (0.327) to the near-critical mean field value (0.5) because when the system is far from the Ising critical point, then it is also far from the mean-field critical point. Thus the description of the coexisting phases for all temperatures becomes a much more difficult problem; one which is only now being worked on.<sup>9</sup> However, we will develop here a simple method to approximately determine the region in reduced temperature over which correction-to-scaling should work.

As fluid mixtures phase separate, they will (a) eventually separate into pure components, (b) approach another critical point, and/or (c) undergo a first-order phase transition. Many of the systems studied in the literature are like the one studied here: the phases asymptotically approach pure components. This is clear in Fig. 2, but is also shown in Fig. 4 by the slope of the curve asymptotically approaching zero. This slope is the effective exponent  $\beta_{\text{eff}}$  and can be calculated by<sup>7</sup>

$$\beta_{\text{eff}} = \frac{\delta \ln(x_u - x_l)}{\delta \ln(t)}. \quad (5)$$

Near the critical point ( $t \rightarrow 0$ ),  $\beta_{\text{eff}}$  is the Ising exponent  $\beta=0.327$ . There have not been theoretical predictions as to the functional form for  $\beta_{\text{eff}}$  as  $t$  gets large, but we will show that  $\beta_{\text{eff}}$  approaches zero exponentially. Singh and Pitzer<sup>7</sup> numerically calculated  $\beta_{\text{eff}}$  from the Ising model and compared that prediction with a curve representing their fit using Eq. (2) to the acetonitrile+cyclohexane data of Vani<sup>25</sup> and also to perfluoroheptane+carbon tetrachloride data of Jacobs.<sup>26</sup> The first two curves are reproduced in Fig. 5 on a plot of  $\beta_{\text{eff}}$  versus the quantity  $(1-t)$ . Singh and Pitzer con-

clude that coexistence curves for liquid-liquid mixtures near an upper consolute point have  $B_1=0$  and  $B_2 < 0$ , which gives a linear shape in this plot. Moreover, they argue that these amplitudes are consistent with correction-to-scaling amplitudes found from susceptibility measurements and with the shape determined by their analysis of the Ising model (see Fig. 5). We have taken numerical derivatives of our coexistence curve data for  $t > 10^{-2}$  and superimposed that data on the curves of Singh and Pitzer. Indeed, a line can be drawn corresponding to  $B_1=0$  and  $B_2=-1.0$  that is consistent with much of our data. However, at temperatures further from critical,  $\beta_{\text{eff}}$  slowly approaches zero, which is quite unlike these lines which will become negative in experimentally accessible regions. It is inappropriate to use correction to scaling, as in Eq. (2), to describe liquid-liquid coexistence

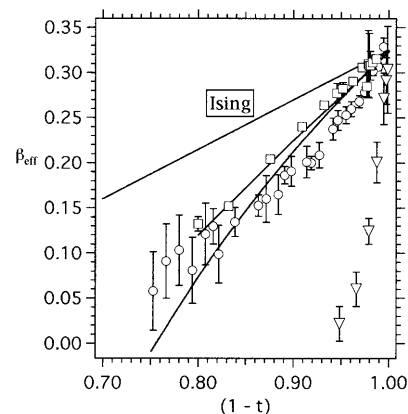


FIG. 5. The effective slope of the data in Fig. 4 as a function of  $(1-t)$ , where  $t$  is the reduced temperature. Close to the critical point,  $\beta_{\text{eff}}$  has the Ising exponent value  $0.327 \pm 0.002$ , but far from critical  $\beta_{\text{eff}}$  approaches zero. The line marked "Ising" is from Ref. 7. The squares are calculated from the acetonitrile-cyclohexane data of Ref. 25, while the line through the squares is the best fit reported in Ref. 7 when two correction-to-scaling terms are used as described in the text. Our data are the circles, and the lowest line is a line with two correction terms ( $B_1=0$  and  $B_2=-1.0$ ) following Ref. 7. The triangles are calculated from the triethylamine-water data of Ref. 27.

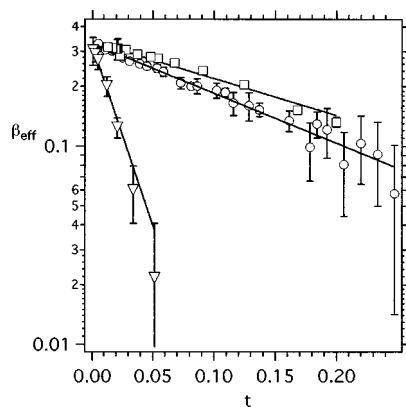


FIG. 6. The effective slope  $\beta_{\text{eff}}$  data shown in Fig. 5 are plotted semi-logarithmically as a function of reduced temperature  $t$ . The data fall on the straight lines shown with slope and intercept given in Table IV and indicate consistency with an exponential approach to zero. The symbols are the same as in Fig. 5.

curve data in a temperature region where  $\beta_{\text{eff}}$  approaches zero and where the system may have crossed over to mean-field behavior.

Instead, we develop an empirical description of  $\beta_{\text{eff}}$  when far from critical. For purposes of comparison, we chose two additional systems, triethylamine+water (T-W) and acetonitrile+cyclohexane (A-C), for which we have available, published coexisting phase data over a large region of  $t$ . The A-C mole fraction data<sup>25</sup> in the region of interest,  $t > 1.4 \times 10^{-2}$ , are analyzed to determine the numerical derivative  $\beta_{\text{eff}}$ , which is shown in Fig. 5. Although the T-W system exhibits a lower consolute point, it has been well studied and is a good comparative system because of the strong hydrogen bonding and the resulting large value of  $B$ . The published density data of Chaar<sup>27</sup> has been converted to volume fraction in order to determine  $\beta_{\text{eff}}$ , which is shown in Fig. 5. Numerical derivatives for all three systems were fitted by a simple exponential approach of  $\beta_{\text{eff}}$  to zero:

$$\beta_{\text{eff}} = \beta e^{-\lambda t}, \quad (6)$$

where  $\beta$  is the Ising exponent (0.327),  $\lambda$  is a system-dependent parameter, and  $t$  is the reduced temperature. The results are shown in Fig. 6 and the parameter values are given in Table IV, where it is shown empirically that  $\lambda \approx (0.6B)^{1/\beta} / \beta \approx 0.64B^{3.07}$  for these systems and will, we

TABLE IV. Parameter values when Eq. (6) is used to fit the numerical derivative,  $\beta_{\text{eff}}$ , in three systems: perfluoromethylcyclohexane-isopropyl alcohol (PFMC-IPA), triethylamine-water (T-W), and acetonitrile-cyclohexane (A-C).

System	$\beta$	$\lambda$	$B$	$(\lambda\beta)^{\beta}/B$
PFMC-IPA	$0.330 \pm 0.005$	$5.8 \pm 0.2$	$2.16 \pm 0.04^a$	$0.57 \pm 0.02$
T-W	$0.325 \pm 0.009$	$42 \pm 4$	$3.90 \pm 0.03^b$	$0.60 \pm 0.02$
A-C	$0.338 \pm 0.005$	$4.3 \pm 0.2$	$1.83^c$	$0.62 \pm 0.02$

<sup>a</sup>From Table III.

<sup>b</sup>Our reanalysis of the density measurements of Ref. 27 converted to volume fraction.

<sup>c</sup>Reference 25.

expect, hold for any liquid-liquid system. It is not surprising that  $\lambda$  is related to  $B$ , since the larger  $B$  is then the smaller  $t$  will be when  $\Delta x$  approaches the limiting value of 1 (pure components). The particular form for  $\lambda(B)$  is suggested by identifying a cutoff reduced temperature  $t_c = B^{-1/\beta}$ , given by simple scaling when  $\Delta x = 1$ , with a characteristic reduced temperature when  $\lambda t_c = 1$  in Eq. (6).

The implications of Eq. (6) for the coexistence curve are easily determined. Very close to the critical point ( $t \ll 1/\lambda$ ), simple scaling results and Eq. (1) follows. Further from the critical point

$$\begin{aligned} \Delta x &= B t^\beta e^{-\lambda \beta t} e^{\beta \lambda^2 t^2 / 4} e^{-\beta \lambda^3 t^3 / 18} \dots \\ &\approx B t^\beta \left( 1 - \lambda \beta t + \frac{\beta(1+2\beta)\lambda^2}{4} t^2 - \dots \right), \end{aligned} \quad (7)$$

where the expansion for small  $t$  resembles a Wegner expansion, Eq. (2), with  $\Delta_1 = 0.5$ ,  $B_1 = 0$ , and  $B_2$  negative, consistent with the observation of Singh and Pitzer.<sup>7</sup> Thus, the observed values for  $B_1$  and  $B_2$  may reflect a crossover region more than true Wegner values. The value of  $B_2 = -\lambda\beta$  that one would calculate does not agree well with the fitted values reported for these systems even when  $B_1 = 0$ , because the expansion in Eq. (7) converges slowly, and the fitted values will also contain a contribution from the true Wegner terms. The Wegner expansion also converges slowly and with parameter values  $B_i$  which are found experimentally to change as different temperature regions are fitted.<sup>25,28</sup> One would expect this when correction terms are no longer adequate to describe the data, which we see as exhibiting crossover to a mean-field critical point. Thus, one needs to fit to data fairly close to the critical point for the true Wegner correction amplitudes to be determined and for one not to see the apparent crossover represented by Eq. (7). It is also possible to estimate the region where the data should be free of crossover effects using Eq. (7): setting the second term in the expansion to, say, 2% of the first, which gives  $t_{\text{max}} \approx (0.1)B^{-3.07} \approx 0.009$  for the PFMC-IPA system studied here. Thus our fits in Table III of the volume fraction, coexistence curve used a temperature region  $t < 0.006$  to determine the amplitudes  $B$  and  $B_1$ , and the exponent  $\beta$ .

#### D. Symmetric coexistence curve

Finally, our coexistence curve data can be transformed into other ‘‘composition’’ variables to see if the curve can be made as symmetric as a simple Ising model. Japas and Levelt Sengers<sup>5</sup> provide a nice definition of such a symmetric curve: (1) simple scaling holds over the largest possible range, (2)  $\beta$  assumes the theoretical value of 0.327, (3) the critical composition is 0.5, and (4) the diameter is a constant except for the  $(1-\alpha)$  anomaly. The critical exponent  $\beta$  is such a well-determined, universal quantity that it is now reasonable to require that this exponent become close to its theoretical value for any composition variable. Japas *et al.* were unable to satisfy even three of these four conditions in their study of the ionic system tetra pentylammonium bromide in water. However, Sanchez<sup>3</sup> could achieve three of the four conditions (critical composition was 0.3 instead of 0.5)

TABLE V. Parameter values corresponding to the best fit of Eq. (9) used to symmetrize the coexistence curve.  $R$  is defined in Eq. (8) and determines the “composition” variable;  $R=1$  is the original volume fraction. The reduced temperature was  $|t| < 6 \times 10^{-3}$  for all these fits.

Fit #	$\psi_c$	$a$	$B$	$\beta$	$R$	$\chi^2/N$
1	0.6210 $\pm 0.0006$	0	2.206 $\pm 0.002$	0.327	1	1.01
2	0.589 $\pm 0.015$	0	2.270 $\pm 0.030$	0.327	1.146 $\pm 0.073$	0.97
3	0.5	0	2.322 $\pm 0.018$	0.327	1.657 $\pm 0.004$	1.43
4	0.5	0	2.46 $\pm 0.08$	0.336 $\pm 0.005$	1.657 $\pm 0.004$	1.39
5	0.5	3.09 $\pm 0.55$	2.350 $\pm 0.020$	0.327	1.648 $\pm 0.004$	0.99

in symmetrizing the polymer solutions resulting from various molecular weight polystyrene in methylcyclohexane. Damay and Leclercq<sup>11</sup> had similar success in symmetrizing the acetonitrile–cyclohexane data of Vani<sup>25</sup> when the critical composition was 0.58.

The transformations to other compositionlike variables all take advantage of the conversions among mole, mass, and volume fractions which have the form:

$$\psi = \frac{\phi}{\phi + R(1 - \phi)}, \quad \phi = \frac{\psi}{\psi + (1 - \psi)/R}, \quad (8)$$

where  $\phi$  is the volume fraction and  $\psi$  is another composition variable. The value of  $R$  determines the composition variable:  $R=1$  is volume fraction,  $R=\rho_2/\rho_1=0.44$  is mass fraction, and  $R=(\rho_2/\rho_1)(M_{w1}/M_{w2})=2.56$  is mole fraction. None of these traditional choices give a completely symmetric coexistence curve as defined above; however,  $R$  can be a free parameter in fitting our coexistence curve data in an attempt to symmetrize the curve. While this has been done previously in various ways,<sup>3,5,11</sup> we choose the following algorithm. A function that describes the upper ( $u, +$ ) and lower ( $l, -$ ) branches of the coexistence curve in the variable  $\psi$  is

$$\psi_{l,u} = \psi_c + at + bt^{1-\alpha} \pm \left(\frac{B}{2}\right) t^{\beta} \pm D' t^{\beta+\Delta_1} \\ \approx \psi_c + at \pm \left(\frac{B}{2}\right) t^{\beta}, \quad (9)$$

where the terms with  $D'$  and  $b$  are negligible close to the critical point, and the ideal values of  $\psi_c$  and  $a$  are 0.5 and 0, respectively. The parameters  $\psi_c$ ,  $a$ ,  $B$ ,  $\beta$ , and  $R$  can be free or fixed at selected values as this function is used to fit the coexistence curve data by calculating a  $\psi$ , and then using Eq. (8) to calculate  $\phi$ , which is compared to the experimental data in Table I for  $t < 6 \times 10^{-3}$ . The near critical coexistence curve data are used to determine the best fit parameter values, which are reported in Table V, in order to assure that the Ising critical point dominates.

A “composition” variable could not be found that provided a more symmetric coexistence curve than that obtained with the volume fraction. Fit 1 in Table V is from Table III when volume fraction ( $R=1$ ) is used and the diameter of the

curve is a constant ( $a=0$ ). The other fits allow certain parameters to vary while holding the rest fixed. Poor fits resulted when the critical composition  $\psi_c$  was fixed at 0.5 unless the diameter could have a slope ( $a \neq 0$ ). When the diameter was a constant, the best fit was with  $R=1.146 \pm 0.073$  and  $\psi_c = 0.589 \pm 0.015$ , but this fit was only slightly better than fit 1 with volume fraction. These two composition

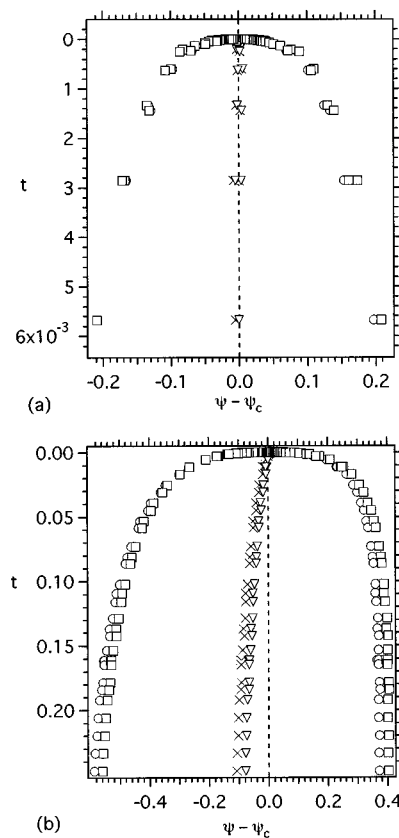


FIG. 7. Coexistence curve plots using either volume fraction (circles) or a calculated composition variable  $\psi$  (squares are using  $R=1.146$ ) from Eq. (8). The  $x$ 's are the diameter of the volume fraction while the  $\nabla$  are the diameter for the  $\psi$  variable: (a) shows the data close to the critical point, where the fits by Eq. (9) are performed as reported in Table V, and (b) shows the data over the entire range of reduced temperatures.



TABLE VI. The diameter in the composition variable  $\psi$  obtained when  $R=1.146$ , which gave the most symmetric coexistence curve in the region near critical (see Table V). The equations used to fit  $\bar{\psi}$ , which is calculated from  $\phi$  using Eq. (8), are equivalent to those used in Table II.  $\bar{\psi}$  is fit over the entire  $10^{-6}<t<0.26$ .

$\bar{\psi} = \psi_c + at + bt^2 + ct^3$ (analytic)					
	$\psi_c$	$a$	$b$	$c$	$\chi^2/N$
	0.5893	-0.567	1.047	0	1.30
	$\pm 0.0003$	$\pm 0.012$	$\pm 0.059$		
	0.5895	-0.645	2.04	-2.94	1.16
	$\pm 0.0003$	$\pm 0.027$	$\pm 0.32$	$\pm 0.93$	
$\bar{\psi} = \psi_c + At^\sigma + A_1t^{\sigma+\Delta_1}$ , $\Delta_1 \equiv 0.5$					
	$\psi_c$	$A$	$A_1$	$\sigma$	$\chi^2/N$
	0.5904	-0.2065	0	0.65	1.80
	$\pm 0.0003$	$\pm 0.0019$			
	0.5903	-0.202	-0.010	0.65	1.83
	$\pm 0.0003$	$\pm 0.009$	$\pm 0.020$		
*	0.5897	-0.511	0.471	0.89	1.24*
	$\pm 0.0003$	$\pm 0.016$	$\pm 0.036$		
	0.5895	-0.71	0.80	0.99	1.19
	$\pm 0.0003$	$\pm 0.11$	$\pm 0.19$	$\pm 0.05$	

variables are compared in Fig. 7, where the difference is barely discernible close to critical where the fits were done, and slightly different over the entire region where data were taken. In Table VI, a series of fits of the diameter data in the composition variable corresponding to  $R=1.146$  are done. These fits can be compared with those given in Table II when using volume fraction, which gave somewhat better fits to the diameter data over the entire temperature region. Moreover, there is not much statistical significance to the difference between the volume fraction and the composition variable with  $R=1.146$ , since the error in  $R$  is just two standard deviations from the volume fraction ( $R=1$ ). We were unable to find a composition variable that would fully symmetrize the coexistence curve using the criteria of Japas *et al.*; however, the volume fraction produced a nearly symmetric coexistence curve about a critical composition  $\phi_c = 0.6210 \pm 0.0006$ .

## V. CONCLUSION

Precise refractive index data on a critical mixture of perfluoromethylcyclohexane and isopropyl alcohol were combined with equally precise refractive index and density measurements on the pure fluids to allow the volume fraction to be calculated from the Lorentz-Lorenz relation. The resulting coexistence curve was as symmetric about the critical composition  $\phi_c = 0.6215 \pm 0.0015$  as any composition variable that can be created using the standard transformation of Eq. (8). The data near the critical point confirmed the theoretical value of the critical exponent  $\beta$  and correction-to-scaling terms could be applied appropriately. A crossover region to a mean-field critical point is suspected and further theoretical research needs to be done to confirm such a crossover. We show that the effective exponent  $\beta_{\text{eff}}$  approaches zero asymptotically as an exponential, and note the difficulties this creates when trying to interpret Wegner, correction-to-scaling amplitudes that are determined by fitting experimental data over a range in temperature that includes a

region where the phases are becoming pure components. By finding an approximately universal approach to such a region, the value of  $\lambda$  can be calculated from the amplitude  $B$  and a region free of crossover can be estimated.

## ACKNOWLEDGMENTS

We thank Stephanie Teemer, Vonda Fairbanks, and Linda King for helpful measurements, and M. A. Anisimov, J. M. H. Levelt Sengers, and S. C. Greer for helpful discussions. This research was supported by NASA Grant No. NAG3-1404.

- J. V. Sengers and J. M. H. Levelt-Sengers, *Annu. Rev. Phys. Chem.* **37**, 189 (1986); S. C. Greer and M. R. Moldover, *ibid.* **32**, 233 (1981).
- A. Kumar, H. R. Krishnamurthy, and E. S. R. Gopal, *Phys. Rep.* **98**, 57 (1983).
- I. C. Sanchez, *J. Appl. Phys.* **58**, 2871 (1985).
- J. Dudowicz, K. F. Freed, and J. F. Douglas, *Macromolecules* **28**, 2276 (1995).
- M. L. Japas and J. M. H. Levelt-Sengers, *J. Phys. Chem.* **94**, 5361 (1990).
- J. Rouch, P. Tartaglia, A. Safouane, and S. H. Chen, *Phys. Rev. A* **40**, 2013 (1989).
- R. R. Singh and K. S. Pitzer, *J. Chem. Phys.* **90**, 5742 (1989).
- M. A. Anisimov, S. B. Kiselev, J. V. Sengers, and S. Tang, *Physica A* **188**, 487 (1992).
- M. A. Anisimov, E. E. Gorodetskii, V. D. Kulikov, A. A. Povodyrev, and J. V. Sengers, *Physica A* **220**, 277 (1995); M. A. Anisimov, A. A. Povodyrev, V. D. Kulikov, and J. V. Sengers, *Phys. Rev. Lett.* **75**, 3146 (1995).
- F. Vnuk, *J. Chem. Soc. Faraday Trans. 2*, **77**, 1045 (1981).
- P. Damay and F. Leclercq, *J. Chem. Phys.* **95**, 590 (1991).
- A. C. Ploplis, P. S. Wardwell, and D. T. Jacobs, *J. Phys. Chem.* **90**, 4676 (1986).
- C. Houessou, P. Guenoun, R. Gastaud, F. Perrot, and D. Beysens, *Phys. Rev. A* **32**, 1818 (1985).
- D. T. Jacobs, *J. Chem. Phys.* **91**, 560 (1989).
- J. V. Sengers, D. Bedeaux, P. Mazur, and S. C. Greer, *Physica A* **104**, 573 (1980); D. Beysens and G. Zalczer, *Phys. Rev. Lett.* **65**, 1690 (1990); C. Pépin, T. K. Bose, and J. Thoen, *ibid.* **65**, 1691 (1990); D. Beysens and G. Zalczer, *Europhys. Lett.* **8**, 777 (1989).
- W. V. Andrew, T. B. K. Khoo, and D. T. Jacobs, *J. Chem. Phys.* **85**, 3985 (1986).
- R. Gastaud, D. Beysens, and G. Zalczer, *J. Chem. Phys.* **93**, 3432 (1990).

- <sup>18</sup>J. W. Schmidt and M. R. Moldover, *J. Chem. Phys.* **83**, 1829 (1985).
- <sup>19</sup>O. Kratky, H. Leopold, and H. Stabinger, *Z. Angew. Phys.* **27**, 273 (1969).
- <sup>20</sup>J. W. Schmidt and M. R. Moldover, *J. Chem. Phys.* **84**, 4563 (1986); **79**, 379 (1983).
- <sup>21</sup>P. R. Bevington, *Data Reduction and Error Analysis for the Physical Sciences* (McGraw-Hill, New York, 1969).
- <sup>22</sup>WaveMetrics, Inc., Lake Oswego, OR 97035.
- <sup>23</sup>W. H. Press, B. P. Flannery, S. A. Teukolsky, and W. T. Vetterling, *Numerical Recipes* (Cambridge University Press, Cambridge, 1986), p. 533.
- <sup>24</sup>K. A. Andrews and D. T. Jacobs (unpublished).
- <sup>25</sup>V. Vani, S. Guha, and E. S. R. Gopal, *J. Chem. Phys.* **84**, 3999 (1986).
- <sup>26</sup>D. T. Jacobs, *J. Phys. Chem.* **86**, 1895 (1982).
- <sup>27</sup>H. Chaar, M. R. Moldover, and J. W. Schmidt, *J. Chem. Phys.* **85**, 418 (1986).
- <sup>28</sup>S. C. Greer, *Phys. Rev. A* **14**, 1770 (1976); A. Bourgou and D. Beysens, *Phys. Rev. Lett.* **47**, 257 (1981).